Outskirts of Galaxy Clusters: Intense Life in the Suburbs
Proceedings IAU Colloquium No. 195, 2004
A. Diaferio, ed.
© 2004 International Astronomical Union
DOI: 10.1017/S1743921304000122

Voids in a ΛCDM universe

Jörg M. Colberg

University of Pittsburgh, 3941 O'Hara Street, 100 Allen Hall, Pittsburgh PA 15260, USA
email: astro@jmcolberg.com

Abstract. We study the formation and evolution of voids in the dark matter distribution using various simulations of the popular Λ Cold Dark Matter Universe. We identify voids by requiring them to be spherical or elliptical regions of space with a mean overdensity of −0.8 or less. The distribution of void sizes in the different simulations shows good overlap. The size of a void is related to the depth of the smoothed density field at that position in the initial conditions. The rescaled mass profiles of voids in the different simulations agree remarkably well. We find a universal void mass profile of the form $\rho(<r)/\rho(r_{\rm eff}) \propto \exp[(r/r_{\rm eff})^{\alpha}]$ where $r_{\rm eff}$ is the effective void radius and $\alpha \sim 2$. The mass function of haloes in voids is steeper than that of haloes which populate denser regions.

1. Introduction

Galaxy redshift surveys show a complicated network of galaxies around large almost empty regions, so-called voids. One of the most famous voids, in the region of Boötes, has a diameter of $\sim 50h^{-1}$Mpc, and was found by Kirschner *et al.* in 1981.† Even though there have been some studies of properties of voids during the 1980s and 1990s (see e.g. Müller *et al.* 2000 and references therein), only recently have galaxy surveys become large enough to yield void samples which allow systematic studies (e.g. Rojas *et al.* 2003).

For similar reasons, voids in cosmological N–body simulations have also been somewhat less well-studied. Early simulations of Cold Dark Matter (CDM) universes showed that large empty regions were generic (Davis *et al.* 1985), and larger, more recent simulations (e.g., Jenkins *et al.* 1998) have provided a clearer picture of voids. Detailed studies of the properties of voids in the dark matter distribution are now becoming increasingly common (e.g. Gardner 2001, Schmidt *et al.* 2001, Gottlöber *et al.* 2003).

One of the problems with studies of voids is that there is little agreement on how to define a void in the galaxy distribution. Are voids regions which are completely devoid of galaxies? If no, how do void-galaxies differ from the galaxies which populate denser environments?

In models of galaxy formation within the context of hierarchical clustering, the galaxy distribution is determined by the underlying dark matter. Therefore, to understand void galaxies, it is important to define precisely what constitutes a void in the dark matter distribution. Dubinski *et al.* (1992) argued that the spherical evolution model (Gunn & Gott 1972) provides a useful guide. Here, we report on the results of a study which uses this definition of voids in the standard cosmology, ΛCDM.

† Throughout this work, we will express the Hubble constant in units of $H_0 = 100h$ km sec^{-1} Mpc^{-1}.

https://doi.org/10.1017/S1743921304000122 Published online by Cambridge University Press

Simulation	Reference	n_p	l $[h^{-1}\text{Mpc}]$	m_p $[10^{10}h^{-1}M_\odot]$
GIF	Jenkins *et al.* 1998	256^3	141.3	1.4
VLS	Jenkins *et al.* 2001	512^3	479	6.9
GIF2	Gao *et al.* 2003	400^3	110	0.2
HV	Evrard *et al.* 2002	1000^3	3000	224.8

Table 1. Parameters of the simulations used in this work. All runs have $\Omega_m = 0.3$, $\Lambda = 0.7$, $n = 1$, $\sigma_8 = 0.9$, $h = 0.7$.

2. Finding voids in Cold Dark Matter universes

2.1. *The simulations*

For the study, we use a set of N–body simulations done by the Virgo Supercomputing Consortium‡. The simulations model regions of different sizes with different mass resolutions. Table 2.1 provides details about the simulations; in the following, we will refer to them as GIF, VLS, GIF2, and HV.

2.2. *The void finding algorithm*

A number of void-finding algorithms have been proposed (see e.g. Kauffmann & Fairall 1991, Aikio & Mähönen 1998, or Hoyle & Vogeley 2002). Most look for empty spherical or cubical regions, which are then usually merged together following some recipe. Our algorithm is a variant of the one advocated by Aikio & Mähönen (1998). It is based on the assumption that voids are primordial negative overdensity perturbations which grew gravitationally and have reached shell–crossing at present time. At shell-crossing, the comoving radius of a perturbation is 1.7 times larger than it was initially, so that the object has a density contrast of -0.8 (see Blumenthal *et al.* 1992, Dubinski *et al.* 1993). Strictly speaking, these numbers are correct for an Einstein de-Sitter cosmology. But the dependence on cosmology is weak, and we ignore it. Our algorithm looks for such regions in the simulations by finding spherical proto-voids first and then merging those so that final voids can be either spherical or have a more complex shape. However, we make sure that we never get configurations where two or more voids are joined through a thin tunnel. Thus, our void finder is analogous to the spherical–overdensity method for dark matter haloes (Lacey & Cole 1994). We compute the center of each void by taking the volume–weighted average of the centers of its constituent spheres. We compute an 'effective' radius by taking the radius of a sphere whose volume matches that of the void.

3. Voids in a ΛCDM universe

3.1. *Visual impression*

Figure 1 gives a visual impression of the voids in the VLS simulation volume at $z = 0$. The image was generated using a ray–tracing programme, rendering the proto–voids as spheres. From the image it is clear that the voids fill almost the entire volume.

3.2. *The void volume function*

On the left–hand side, Figure 2 shows the number density of voids larger than a given volume at $z = 0$ in the four simulations. Note that there is not a single very big void in the GIF simulations. The curves obtained from the different simulations show very good

‡ http://www.virgo.dur.ac.uk

https://doi.org/10.1017/S1743921304000122 Published online by Cambridge University Press

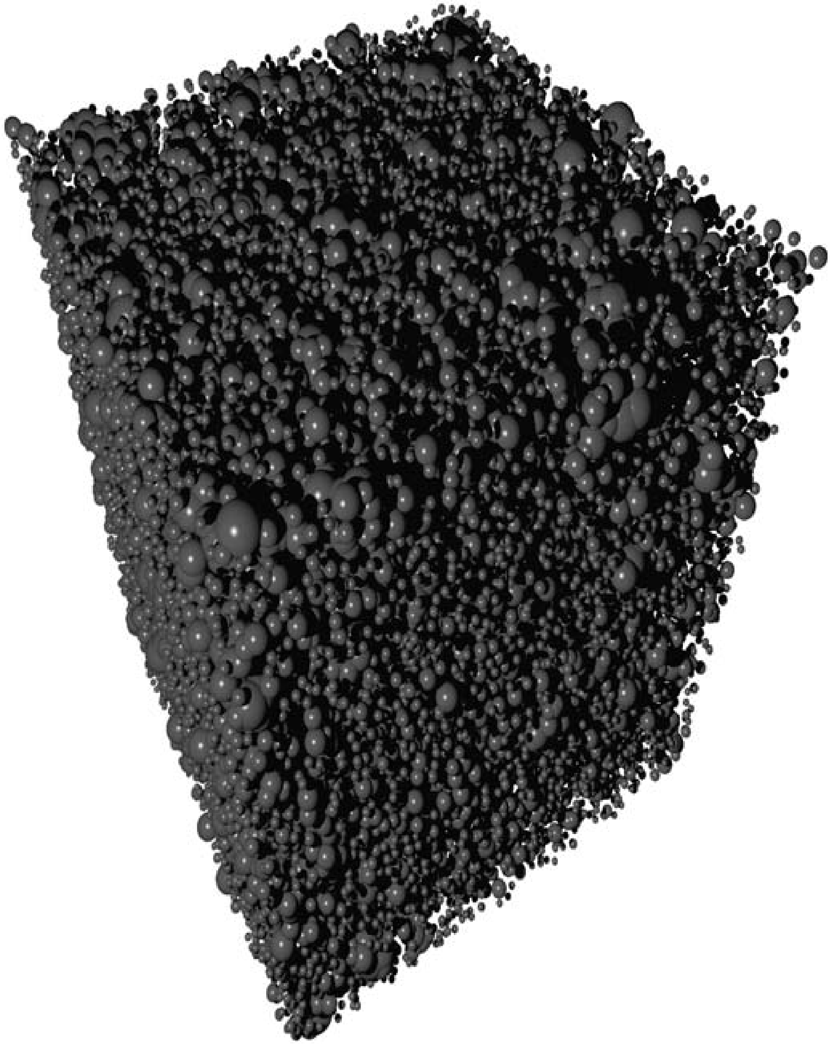

Figure 1. Voids in the VLS simulation at $z = 0$.

overlap. The steps visible at small V result from the discreteness of the grid. The largest void found in the HV simulation has an effective radius of $55\,\mathrm{Mpc}/h$.

On the right–hand side, Figure 2 shows how the cumulative volume function in the highest resolution simulation (GIF2) evolves. The evolution is smooth, and the volume functions at different redshifts cross each other.

3.3. *Voids in the initial density field*

Massive haloes in simulations are associated with higher peaks in the (smoothed) initial density field (Bardeen *et al.* 1986; Colberg *et al.* 2000). Voids are expected to form from initially underdense regions analogously to how clusters or haloes form from initially overdense regions. So one might wonder if a similar correlation exists between voids and minima in the initial density field. We used the GIF simulations to study this correlation.

https://doi.org/10.1017/S1743921304000122 Published online by Cambridge University Press

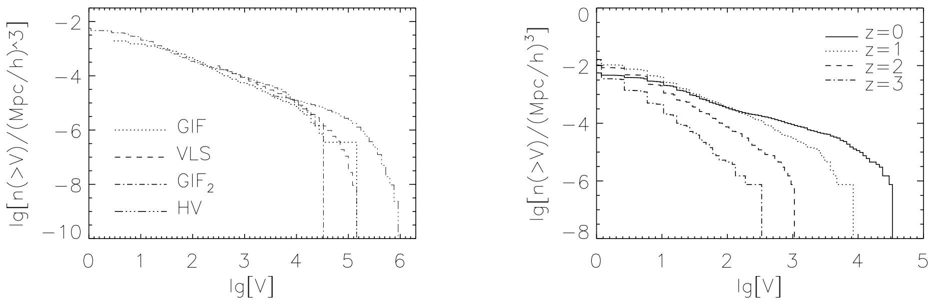

Figure 2. Left: Cumulative volume functions of voids at $z = 0$ in the GIF2 (dot–dashed), GIF (dotted), VLS (dashed), and HV simulations (dot-dot-dot-dashed). Right: Evolution of the the cumulative void volume fraction in the GIF2 simulation at $z = 0$ (solid), $z = 1$ (dotted), $z = 2$ (dashed), and $z = 3$ (dot–dashed).

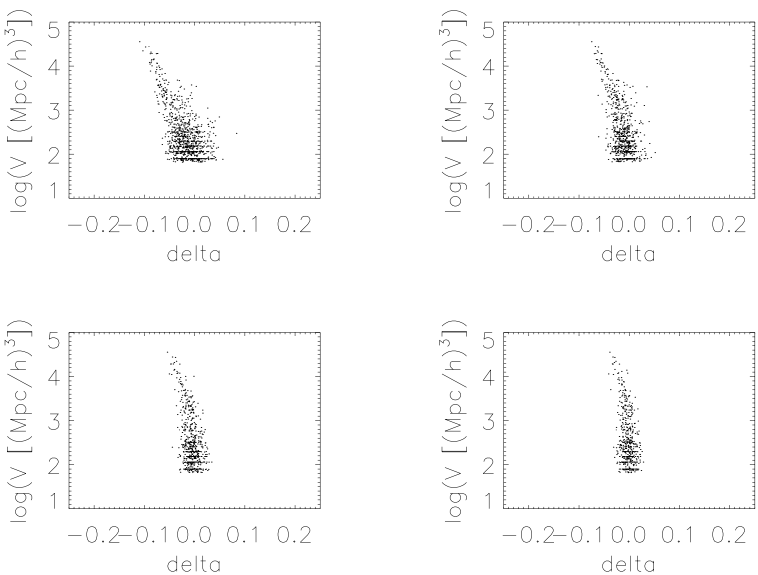

Figure 3. Voids in the smoothed GIF initial density field. There is a correlation between the void volume at $z = 0$, and the underdensity δ of the associated minimum in the initial field. Different panels show results for different smoothing scales: $5.0h^{-1}$Mpc (upper left), $7.5h^{-1}$Mpc (upper right), $10.0h^{-1}$Mpc (bottom left), and $12.5h^{-1}$Mpc (bottom right).

Since the voids in our sample enclose a large range of masses, we smoothed the initial ($z = 49$) density field using a set of four Top Hat filters: 5.0, 7.5, 10.0, and $12.5h^{-1}$Mpc. We identified the minima in each smoothed field and, where possible, associated a void with it. Where there are two or more minima for one void we pick the deepest one. Not all voids had associated troughs, but this is not very surprising, since Colberg *et al.* did not find a peak for each cluster either.

Figure 3 shows the results for the four smoothing scales. All four panels show the void volumes as a function of the overdensities of the associated troughs. Most of the voids can be associated with troughs in the initial density field. Larger voids form from somewhat deeper troughs than smaller voids, and there is a correlation between the size of a void

https://doi.org/10.1017/S1743921304000122 Published online by Cambridge University Press

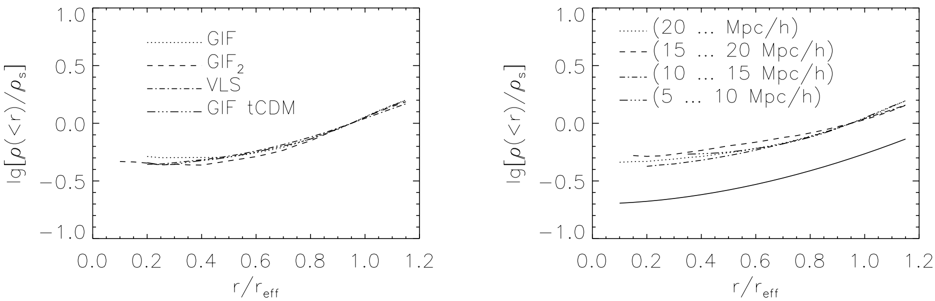

Figure 4. Left: Enclosed density in $z = 0$ voids as a function of radius for the GIF2 (dashed line), GIF (dotted line), and VLS (dot–dashed line) simulations (averaged over voids with $r_{eff} > 5\,\mathrm{Mpc}/h^{-1}$). In addition, the results from the $\Omega = 1$ τCDM GIF simulation are shown (three dots–dashed line). Curves are truncated at small radii because of the numerical resolution limits. Right: Enclosed density profiles in the VLS simulation, using four samples with void radii between 5 and $10h^{-1}$Mpc (dashed-three-dots), 10 and $15h^{-1}$Mpc (dot dashed), 15 and $20h^{-1}$Mpc (dashed), and voids with radii larger than $20h^{-1}$Mpc (dotted), averaged over all voids in each sample. Solid line shows equation (3.1), but shifted downwards by a factor of two.

and the depth of its corresponding trough, although this correlation is fairly weak for small voids.

3.4. *Void density profiles*

Navarro *et al.* (1996) have argued that CDM haloes have a universal density profile. We argue that the same holds true for voids.

Using our samples from the GIF, GIF2, and VLS simulations, we have computed the mass profiles of voids. On the left–hand side of Figure 4 we show the averaged enclosed density in $z = 0$ voids as a function of radius. For each void, we re–scaled the length scales (densities) by dividing by the effective radius (enclosed density at that radius). For almost the entire range, the average density profiles of voids in the three simulation sets agree very well. We also computed density profiles for the $\Omega = 1$ τCDM GIF simulation. These agree with the profiles of the ΛCDM simulations. This finding indicates that the form of void density profiles is indeed universal.

The cumulative profile shown in Figure 4 is quite well described by

$$\rho(< r)/\rho(r_{\rm eff}) = \frac{\exp[(r/r_{\rm eff})^{1.85}]}{2.5}\,. \qquad (3.1)$$

3.5. *The void halo mass function*

We study the mass function by using the GIF2 simulation which has the highest mass resolution. We identify haloes using a friends–of–friends (fof) group finder with a linking length of 0.2 times the mean interparticle separation. At $z = 0$, we find void haloes by picking those haloes whose centres-of-mass lie within a void. We then mark those particles that are in a void at $z = 0$ and run the fof group finder on them at earlier redshifts.

Figure 5 compares the mass function of all haloes with that of haloes whose particles lie in a void at $z = 0$. The plot indicates that haloes which end up in a void at $z = 0$ – probably located at the very edges of a void – *at any fixed mass* undergo slightly more evolution than haloes with the same mass elsewhere. It also agrees with the more detailed investigation into this topic done by Gottlöber *et al.* (2003) who described the difference between the void and non–void haloes in much detail.

https://doi.org/10.1017/S1743921304000122 Published online by Cambridge University Press

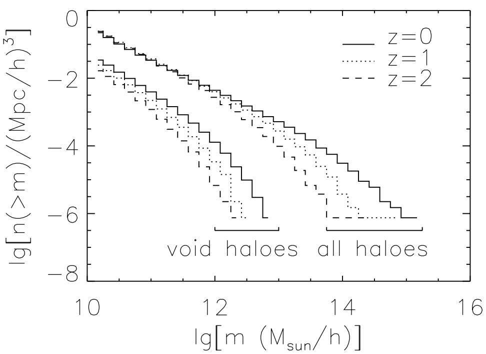

Figure 5. Mass function of haloes in the GIF2 simulation. Different curves show the mass function of all haloes, whatever their surrounding environment, and the mass function of those haloes whose particles lie in a void at $z = 0$.

4. Summary

We discussed the properties of voids in a set of large high-resolution N-body simulations of the ΛCDM cosmology, defining voids as spherical or elliptical regions of space with a mean overdensity of −0.8. The void volume functions of the different simulations agree well. There are more smaller voids at earlier times than at later times. Claims that CDM cosmologies do not form large enough voids can be put to rest given the sizes of the largest voids found in the Hubble Volume simulation. In addition, as our voids are defined through their mean overdensity we also show that CDM voids do not contain too much matter.

Voids correspond to troughs in the initial density field. There is a weak correlation of void size with initial density, larger voids form from somewhat deeper troughs than small voids.

When appropriately rescaled, voids appear to have a universal density profile. The void density profiles rise steeply at the edges of voids. Voids are thus very well defined in terms of their densities.

The mass function of haloes in voids is different from that in regions of average density, it is steeper in voids.

Acknowledgments

I thank my collaborators Ravi Sheth, Antonaldo Diaferio, Liang Gao, Naoki Yoshida, and Adrian Jenkins for allowing me to present the work. The simulations were carried out as part of the Virgo Consortium programme, at the Rechenzentrum of the Max–Planck-Gesellschaft in Garching, Germany and at the Edinburgh Parallel Computing Center.

I also want to thank the organizer of the conference, Antonaldo Diaferio, for enabling such a productive and stimulating workshop.

References

Aikio J. & Mähönen P., 1998 *ApJ* **497**, 534ff.

Blumenthal G. R., Da Costa L, N., Goldwirth D. S., Lecar M., Piran T., 1992 *ApJ* **388**, 234ff.

https://doi.org/10.1017/S1743921304000122 Published online by Cambridge University Press

Colberg J. M., White S. D. M. MacFarland T. J., Jenkins A., Pearce F. R., Frenk C. S., Thomas P. A., Couchman H. M. P. (The Virgo Consortium), 2000 *MNRAS* **313**

Davis M., Efstathiou G., Frenk C.S., White S.D.M., 1985 *ApJ* **292**, 371ff.

Dubinski J., Da Costa L, N., Goldwirth D. S., Lecar M., Piran T., 1993 *ApJ* **410**, 458ff.

Evrard A. E., MacFarland T. J., Couchman H. M. P., Colberg J. M., Yoshida N., White S. D. M., Jenkins A., Frenk C. S., Pearce F. R., Peacock J. A., Thomas P. A., 2002 *ApJ* **573**, 7ff.

Gao L., White S. D. M. and The Virgo Consortium, 2004 *in preparation*

Gardner J.P, 2001 *ApJ* **557**, 616ff.

Gottlöber S., Lokas E., Klypin A., Hoffman Y. *astro-ph/0305393*

Hoyle F., Vogeley M. S., 2002 *ApJ* **566**, 641ff.

Jenkins A., Frenk C. S., Pearce F. R., Thomas P. A., Colberg J. M., White S. D. M., Couchman H. M. P., Peacock J. A., Efstathiou G., Nelson, A. H. (The Virgo Consortium), 1998 *ApJ* **499**, 20ff.

Jenkins A., Frenk C. S., White S. D. M., Colberg J. M., Cole S., Evrard A. E., Couchman H. M. P., Yoshida N., 2001 *MNRAS* **321**, 372ff.

Kauffmann G., Fairall A. P., 1991 *MNRAS* **248**, 313ff.

Kauffmann G., Colberg J. M., Diaferio A., White S. D. M., 1999 *MNRAS* **303**, 188ff.

Lacey C., Cole, S., 1994 *MNRAS* **271**, 676ff.

Müller V., Arbabi–Bidgoli S., Einasto J., Tucker D., 2000 *MNRAS* **318**, 280ff.

Navarro J. F., Frenk C. S., White S. D. M., 1996 *ApJ* **462**, 563ff.

Peebles P. J. E., 2001 *ApJ* **557**, 495ff.

Rojas R.R., Vogeley M.S., Hoyle F., Brinkmann J. *astro-ph/0307274*

Schmidt J.D., Ryden B.S., Melott A.L., 2001 *ApJ* **546**, 609ff.

https://doi.org/10.1017/S1743921304000122 Published online by Cambridge University Press